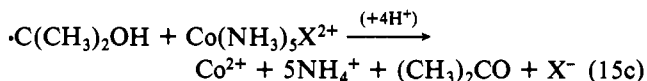
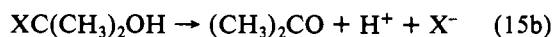
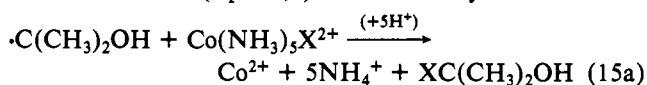
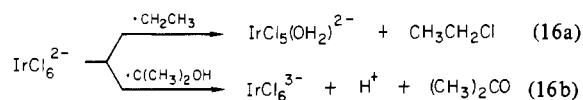


atom abstraction (eq 15a,b) rather than by direct electron



transfer (eq 15c). Caution is particularly warranted considering that reduction of IrCl_6^{2-} by aliphatic radicals proceeds by two pathways,¹¹ the former predominating for alkyl radicals

(e.g., $\cdot\text{CH}_2\text{CH}_3$, eq 16a) and the latter for $\alpha\text{-OH}$ and $\alpha\text{-OR}$ radicals (eq 16b).



Acknowledgment. This research was supported by the Chemical Sciences Division of the Office of Basic Energy Sciences, U.S. Department of Energy, under Contract W-7405-ENG-82. Numerous suggestions and discussions with Dr. A. Bakač are gratefully acknowledged.

Registry No. $\text{Co}(\text{NH}_3)_5\text{F}^{2+}$, 15392-06-0; $\cdot\text{C}(\text{CH}_3)_2\text{OH}$, 5131-95-3; $\cdot\text{CH}(\text{CH}_3)\text{OC}_2\text{H}_5$, 2229-06-3.

(11) (a) Chen, J. Y.; Gardner, H. C.; Kochi, J. K. *J. Am. Chem. Soc.* 1976, 98, 6150. (b) Steeken, S.; Neta, P. *Ibid.* 1982, 104, 1244.

Contribution from the Department of Chemistry, University of Glasgow, Glasgow G12 8QQ, Scotland, U.K.

Kinetics and Mechanism of Reduction of a Nickel(IV) Oxime-Imine Complex by $\text{Co}(\text{edta})^{2-}$. Stereospecific Synthesis of a Stereoselective Oxidant

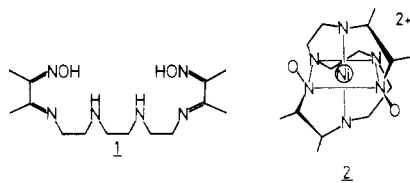
A. GRAHAM LAPPIN,* MAURO C. M. LARANJEIRA, and ROBERT D. PEACOCK

Received June 18, 1982

Kinetics and mechanism of the $\text{Co}(\text{edta})^{2-}$ reduction of a nickel(IV) oxime-imine complex, $\text{Ni}^{\text{IV}}\text{L}^{2+}$, are reported at 25.0 °C and 0.10 M ionic strength. The initial reaction involves outer-sphere electron transfer to form a nickel(III) intermediate, $\text{Ni}^{\text{III}}\text{L}^+$, with a second-order rate constant of $36 \text{ M}^{-1} \text{ s}^{-1}$. The protonated ($\text{p}K_{\text{H}} = 4.07$) form of the intermediate, $\text{Ni}^{\text{III}}\text{LH}^{2+}$, forms a hydrogen-bonded complex with $\text{Co}(\text{edta})^{2-}$ ($K = 480 \text{ M}^{-1}$) through which a second electron transfer ($k = 4 \times 10^{-2} \text{ s}^{-1}$) takes place to give the nickel(II) product. A minor pathway with disproportionation of $\text{Ni}^{\text{III}}\text{L}^+$ is also detected. Stereospecific synthesis of a methylated nickel(IV) derivative, $\text{Ni}^{\text{IV}}((S)\text{-Me}_2\text{L})^{2+}$, is reported, and its properties are compared with those of the partially resolved $\text{Ni}^{\text{IV}}\text{L}^{2+}$ complex. The methylated reagent has been used to investigate stereoselectivity in the reaction with $\text{Co}(\text{edta})^{2-}$. Both nickel(IV) and nickel(III) reactions show an excess of (+)- $\text{Co}(\text{edta})^-$ over (-)- $\text{Co}(\text{edta})^-$ products of around 10%.

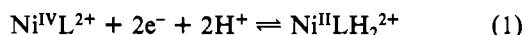
Introduction

Oxime complexes of nickel possess extensive redox chemistry, and there are many reports¹ of species with formal metal ion oxidation states higher than nickel(II). The hexadentate di(oxime-imine) ligand 3,14-dimethyl-4,7,10,13-tetraaza-hexadeca-3,13-diene-2,15-dione dioxime (H_2L (1)) used by



Chakravorty and co-workers² is of particular interest since it allows formation in aqueous media of a long-lived complex that is formally nickel(IV). This complex ($\text{Ni}^{\text{IV}}\text{L}^{2+}$ (2)) forms with oxime deprotonation from the corresponding nickel(II) complex ($\text{Ni}^{\text{II}}\text{LH}_2^{2+}$) and is diamagnetic² and substitution inert,^{2,3} consistent with a low-spin d^6 electronic configuration. It can be optically resolved.³

The nickel(IV) complex undergoes^{4,5} a single reversible two-electron reduction at $\text{pH} < 5$ (eq 1), with a potential of



0.94 V (vs. NHE, the normal hydrogen electrode) while above this pH the intermediate trivalent state can be detected.

Relevant potentials are 0.65 V for eq 2, 0.64 V for eq 3, and 0.42 V for eq 4, all at 25 °C and in $0.10 \text{ mol dm}^{-3} \text{ NaNO}_3$ media.⁵



The low substitution lability and moderately high reduction potential of $\text{Ni}^{\text{IV}}\text{L}^{2+}$ are likely to result in outer-sphere electron-transfer mechanisms. Molecular structure data^{6,7} on related complexes indicate that no major geometry change accompanies reduction of nickel(IV) to nickel(II), and an outer-sphere two-electron transfer was considered a possibility.⁸ However, reduction of nickel(IV) by well-characterized one-⁵ and two-electron⁸ reagents involves consecutive electron transfer and formation of a nickel(III) intermediate.

- (1) Nag, K.; Chakravorty, A. *Coord. Chem. Rev.* 1980, 33, 87.
- (2) Mohanty, J. G.; Singh, R. P.; Chakravorty, A. *Inorg. Chem.* 1975, 14, 2178.
- (3) Heaney, P. J.; Lappin, A. G.; Peacock, R. D.; Stewart, B. *J. Chem. Soc., Chem. Commun.* 1980, 769.
- (4) Mohanty, J. G.; Chakravorty, A. *Inorg. Chem.* 1976, 15, 2912.
- (5) Lappin, A. G.; Laranjeira, M. C. M. *J. Chem. Soc., Dalton Trans.* 1982, 1861.
- (6) Korvenranta, J.; Saarinen, H.; Näsäkkälä, E. *Finn. Chem. Lett.* 1979, 81.
- (7) Saarinen, H.; Korvenranta, J.; Näsäkkälä, E. *Acta Chem. Scand. Ser. A* 1980, A34, 443.
- (8) Lappin, A. G.; Laranjeira, M. C. M.; Youde-Owei, L. *J. Chem. Soc., Dalton Trans.* 1981, 721.

* To whom correspondence should be addressed at the Department of Chemistry, University of Notre Dame, Notre Dame, IN 46556.

A further interesting possibility involves the use of optically active nickel(IV) complexes as potential stereoselective electron-transfer agents. Stereoselectivity has previously been observed in electron-transfer reactions though detection is difficult if there is racemization by electron exchange with a labile redox form of the reagents.⁹ A suitable reductant for stereoselectivity studies with nickel(IV) is $\text{Co}(\text{edta})^{2-}$ ($E^\circ = 0.40 \text{ V}$),¹⁰ which can be oxidized by both nickel(IV) and nickel(III) to give substitution-inert $\text{Co}(\text{edta})^-$. The self-exchange rate of $\text{Co}(\text{II})/\text{Co}(\text{III})$ is very low ($4.0 \times 10^{-7} \text{ M}^{-1} \text{ s}^{-1}$).¹¹

In this paper, the kinetics and mechanism of reduction of $\text{Ni}^{\text{IV}}\text{L}^{2+}$ by $\text{Co}(\text{edta})^{2-}$ are reported. Stereoselectivity in this reaction has been investigated by using a novel optically active nickel(IV) complex, and the stereospecific synthesis of this complex is presented.

Experimental Details

(a) Preparation of $\text{Ni}^{\text{II}}\text{LH}_2(\text{ClO}_4)_2$, $\text{Ni}^{\text{III}}\text{L}(\text{ClO}_4)$, and $\text{Ni}^{\text{IV}}\text{L}(\text{ClO}_4)_2$. The nickel(II) and nickel(IV) complexes with **1** were obtained as perchlorate salts by methods outlined previously.^{2,8} Solutions of nickel(IV) were standardized spectrophotometrically with use of the following literature molar absorptivities: λ (nm, ϵ , $\text{M}^{-1} \text{ cm}^{-1}$) 500 (6300), 430 (5960). Partial optical resolution of the nickel(IV) complex, $\text{Ni}^{\text{IV}}\text{L}^{2+}$, was achieved by chromatography on SP Sephadex cation-exchange resin using potassium (+)-antimonyl tartrate solution ($0.025 \text{ mol dm}^{-3}$) as eluent. The resolved complex was reabsorbed on cation-exchange resin, and the column was washed with water to remove the optically active eluent and eluted with NaClO_4 (0.10 M).

The nickel(III) complex was generated electrochemically by oxidation of $\text{Ni}^{\text{II}}\text{LH}_2^{2+}$ with a flow system¹² with a graphite-powder working electrode packed in a porous glass column and wrapped externally with a Pt-wire electrode. Typically oxidation of a millimolar solution at pH 6 was achieved with use of a flow rate of 2 mL min^{-1} at 0.40 V (vs. Ag/AgCl).

(b) Preparation of (5S,12S)-4,7,10,13-Tetraaza-3,5,12,14-tetramethylhexadeca-3,13-diene-2,15-dione Dioxime, (S)- Me_2LH_2 . The tetraamine (2S,9S)-2,9-diamino-4,7-diazadecane was prepared by the method of Job and Bruce¹³ and was purified by distillation under vacuum (0.5 mmHg, 170–190 °C) to yield a viscous, colorless liquid.

The amine (17.4 g, 0.1 mol) was added to 20.2 g (0.2 mol) of 2,3-butanedione oxime (Sigma) in 250 mL of dry ether and refluxed for 30 min.¹⁴ The impure product, obtained as an oil after removal of solvent, was not purified but used in a crude state to form metal complexes.

(c) Preparation of $\text{Ni}^{\text{II}}((\text{S})\text{-Me}_2\text{LH}_2)(\text{NO}_3)_2$. The ligand (S)- Me_2LH_2 (6.8 g, 0.02 mol) was added to an ethanolic solution containing 5.8 g (0.02 mol) of nickel(II) nitrate hexahydrate (BDH AnalaR), which was warmed and stirred continuously. The solution turned dark brown. Small amounts of an insoluble pink nickel complex with unreacted oxime impurity were removed by filtration, and the solvent was removed under reduced pressure until brown crystals of $\text{Ni}^{\text{II}}((\text{S})\text{-Me}_2\text{LH}_2)(\text{NO}_3)_2(\text{H}_2\text{O})_2$ formed. Recrystallization from ethanol gave an overall yield of around 30%. Anal. Calcd: Ni, 10.6; C, 34.3; H, 6.4; N, 20.0. Found: Ni, 10.2; C, 33.8; H, 6.6; N, 20.1. The perchlorate salt was prepared by addition of a concentrated ethanolic solution of NaClO_4 to an ethanolic solution of the nitrate salt.

(d) Preparation of $\text{Ni}^{\text{IV}}((\text{S})\text{-Me}_2\text{L})^{2+}$. Two preparative methods were used for this complex, which was not obtained as a crystalline solid. The most convenient method involved addition of 5 mL of concentrated nitric acid to 2 g of $\text{Ni}^{\text{II}}((\text{S})\text{-Me}_2\text{L})(\text{NO}_3)_2$ at 0 °C. After evolution of brown nitrous fumes had ceased, the deep red solution of the nickel(IV) salt was diluted to 10 times its volume and was absorbed on SP Sephadex cation-exchange resin. After the column was washed with distilled water, chromatographically pure $\text{Ni}^{\text{IV}}((\text{S})\text{-Me}_2\text{L})^{2+}$ was obtained by elution with NaClO_4 solution (0.10

M). Elution with potassium (+)-antimonyl tartrate solution (0.025 M) was also carried out.

The alternative method involved chromatographic purification of the nickel(II) complex on SP Sephadex cation-exchange resin, with elution with 0.10 M NaClO_4 solution followed by controlled-potential electrolysis, described previously.

The extinction coefficient of $\text{Ni}^{\text{IV}}((\text{S})\text{-Me}_2\text{L})^{2+}$ was determined at pH 4.02 in acetate buffer and 0.10 M NaClO_4 by quantitative reduction with quinol (BDH AnalaR), which has been shown to react stoichiometrically with nickel(IV) complexes.¹⁵

(e) Preparation of $\text{Co}(\text{edta})^{2-}$. (1,2-Diaminoethane-*N,N,N',N'*-tetraacetato)cobaltate(II), $\text{Co}(\text{edta})^{2-}$, was prepared in situ by adding a stoichiometric amount of $\text{Na}_2\text{H}_2\text{edta}$ (BDH AnalaR) to a previously standardized solution of cobalt(II) nitrate (BDH AnalaR).

(f) Cyclic Voltammetry Studies. Cyclic voltammetry measurements were made in $1.0 \times 10^{-2} \text{ M}$ buffer solutions at an ionic strength of 0.10 M (NaClO_4) and at 25.0 ± 0.1 °C with either the nickel(II) or the nickel(IV) complex at $5 \times 10^{-4} \text{ M}$ concentration. A three-electrode system consisting of a platinum or carbon-paste working electrode, a platinum-wire auxiliary electrode, and a Ag/AgCl (NaCl) reference electrode was used. Voltammograms were generated with use of a Princeton Applied Research Corp. Model 173 potentiostat in conjunction with a Model 175 universal programmer and a Model 176 current to voltage converter and were recorded on a J. J. Lloyd Ltd. PL51 X-Y recorder.

(g) Kinetic Measurements. Kinetic measurements were made in $1.0 \times 10^{-2} \text{ M}$ buffer at an ionic strength of 0.10 M (NaNO_3). Experiments were run under pseudo-first-order conditions with an excess of $\text{Co}(\text{edta})^{2-}$. The pH was varied from 3.5 to 8.0 and was determined immediately after reaction with an E.I.L. 7055 pH meter. A saturated calomel (NaCl) reference electrode was used, and hydrogen ion concentrations were evaluated by using the relationship $-\log [\text{H}^+] = \text{pH} - 0.02$, correcting for both hydrogen ion activity and the liquid-junction potential.

Reactions were monitored at the absorption maximum of the nickel(IV) complex at 500 or 391 nm with use of, for fast reactions ($t_{1/2} < 1 \text{ min}$), an Applied Photophysics stopped-flow spectrometer thermostated at 25.0 ± 0.1 °C. For slower reactions ($t_{1/2} > 1 \text{ min}$), a Beckman 5270 spectrophotometer with a cuvette thermostated at 25.0 ± 0.1 °C was used. In these experiments, 2.5 mL of a $\text{Co}(\text{edta})^{2-}$ solution of known concentration was placed in a 1-cm cell and a drop of standard nickel(IV) solution was added with thorough mixing with a small glass spoon. The $\text{Co}(\text{edta})^{2-}$ concentrations were corrected by the total volume of the solutions in the cell.

Absorbance changes at 500 nm were biphasic over the whole pH range, each phase accounting for approximately 50% of the total change. Where the time constants for the phases were sufficiently well separated, they were analyzed independently. However, in some instances, the reaction rates were not well separated and data for the slower reaction were collected over the second half of the reaction at 391 nm, which is an isosbestic point for the fast process. Under these conditions, both reactions were first order and a consecutive reaction curve fitting treatment¹⁶ was used to determine the rate constant for the faster process with use of data obtained at 500 nm. Reactions using the electrogenerated nickel(III) complex, $\text{Ni}^{\text{III}}\text{L}^+$, under these conditions were monitored at 500 and 391 nm. In both cases reactions showed good first-order behavior with good agreement between the studies at different wavelengths. Observed rate constants were evaluated by least-squares analysis of appropriate plots with a P.E.T. 2001 microcomputer. Normally three rate determinations were made for each kinetic experiment. Linear regression techniques, with weighting of k_{obs}^{-1} where appropriate, were employed for data analysis.

(h) Reaction Stoichiometry and Product Analysis. The stoichiometry of the reaction was determined by addition of aliquots of $\text{Co}(\text{edta})^{2-}$ to a standard $\text{Ni}^{\text{IV}}\text{L}^{2+}$ solution at pH 4.02 and 0.10 M ionic strength. The nickel(IV) solution was then restandardized. Reaction products were separated by chromatography on Sephadex anion-exchange resin and identified spectrophotometrically.

(i) Stereoselectivity and Circular Dichroism Studies. The stereoselectivity of the reduction of $\text{Ni}^{\text{IV}}((\text{S})\text{-Me}_2\text{L})^{2+}$ by $\text{Co}(\text{edta})^{2-}$ was determined under a variety of conditions by measuring the optical

(9) Geselowitz, D. A.; Taube, H. *J. Am. Chem. Soc.* **1980**, *102*, 4525.

(10) Wilkins, R. G.; Yelin, R. E. *Inorg. Chem.* **1968**, *7*, 2667.

(11) Im, Y. A.; Busch, D. H. *J. Am. Chem. Soc.* **1961**, *83*, 3357.

(12) Clark, B. R.; Evans, D. H. *J. Electroanal. Chem. Interfacial Electrochem.* **1976**, *69*, 181.

(13) Job, R. C.; Bruce, T. C. *J. Am. Chem. Soc.* **1974**, *96*, 809.

(14) Ablov, A. V.; Belichuk, N. I.; Kaftanat, V. N. *Russ. J. Inorg. Chem. (Engl. Transl.)* **1972**, *17*, 392.

(15) Lannon, A. M.; Lappin, A. G.; Laranjeira, M. C. M.; Munn, S. F., to be submitted for publication.

(16) Frost, A. A.; Pearson, R. G. "Kinetics and Mechanism", 2nd ed.; Wiley: New York, 1961; p 166.

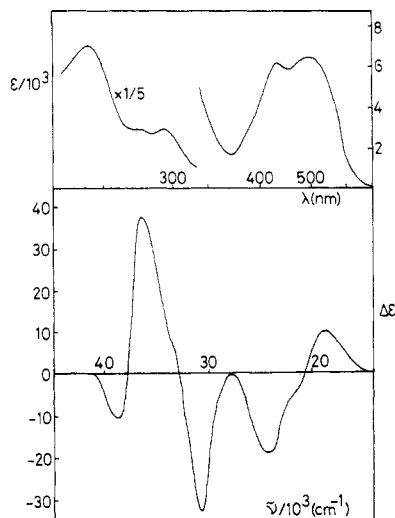


Figure 1. Absorption and circular dichroism spectra of the first eluted isomer of $\text{Ni}^{\text{IV}}\text{L}^{2+}$ in an aqueous solution containing 0.10 M sodium perchlorate.

activity of $\text{Co}(\text{edta})^-$ produced in the reaction. After the appropriate extent of the reaction, solutions were absorbed on DEAE Sephadex anion-exchange resin, the column was washed, and the $\text{Co}(\text{edta})^-$ solutions were eluted with 1.0 M sodium perchlorate solution. Circular dichroism spectra were measured on an instrument comprising a Xenon arc source, a Jobin-Yvonne 0.6M monochromator, a Morvue photoelastic modulator, and a Bentham lock-in amplifier. The instrument was calibrated against an aqueous solution of $\Delta(+)\text{-Co}(\text{en})_3\text{Cl}_3$ ($\Delta\epsilon_{493} = 1.90 \text{ M}^{-1} \text{ cm}^{-1}$).¹⁷

The percentage resolution was determined by comparison with an authentic sample of $\text{K}[(+)\text{-Co}(\text{edta})]^-$ ($\Delta\epsilon -1.79$ (583 nm) and $\Delta\epsilon +0.88$ (500 nm), ϵ 347).

Results and Discussion

(a) Resolution of $\text{Ni}^{\text{IV}}\text{L}^{2+}$. Chromatography of $\text{Ni}^{\text{IV}}\text{L}^{2+}$ on SP Sephadex cation-exchange resin suggests that only one geometric isomer of the complex is formed. Elution with (+)-antimonyl tartrate solution gave a single broad band, and the CD spectrum of the first eluted fraction is shown in Figure 1. The relative intensity of the CD spectrum decreased and changed sign with subsequent band fractions but did not change in form. The complex $\text{Ni}^{\text{IV}}\text{L}^{2+}$ is optically stable and decomposes over several days without racemization.

The two intense absorption bands at 500 nm ($6300 \text{ M}^{-1} \text{ cm}^{-1}$) and 430 nm ($5960 \text{ M}^{-1} \text{ cm}^{-1}$) in the visible region can be assigned as ligand-to-metal charge-transfer transitions.¹⁸ Their dissymmetry factors, $\Delta\epsilon/\epsilon$ ($\sim 3 \times 10^{-3}$), which are similar to those of well-established charge-transfer transitions of diimine complexes,¹⁹ support this assignment. Ligand transitions are likely to be at higher energy. If the shoulder around 300 nm is assigned as the lowest energy ligand transition, the CD spectrum shows a clear exciton couplet in this region. Although assignment of absolute configuration cannot be made with any certainty, it is likely that this absorption, due to the interaction of the two long axis polarized transitions of the ligand oxime-imine groups, is consistent with the configuration shown in 2.

Neither nickel(II) nor nickel(III) complexes with this ligand could be resolved. Indeed, no metal ion optical activity could be detected in a solution of $\text{Ni}^{\text{II}}\text{LH}_2^{2+}$ prepared from the resolved $\text{Ni}^{\text{IV}}\text{L}^{2+}$ freshly reduced by ascorbate ion at pH 4.0. This presents a problem for studies of the stereoselectivity of reactions of $\text{Ni}^{\text{IV}}\text{L}^{2+}$ since electron-transfer-induced racemi-

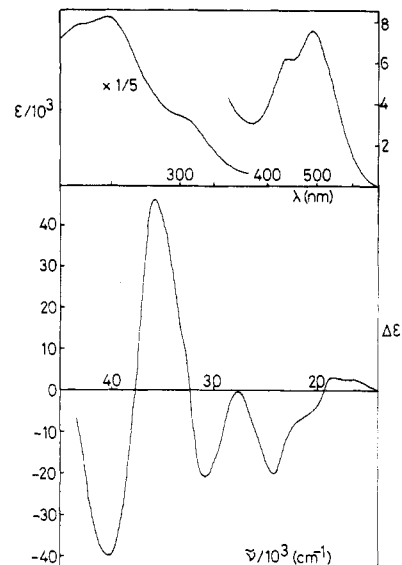


Figure 2. Absorption and circular dichroism spectra of $\text{Ni}^{\text{IV}}((S)\text{-Me}_2\text{L})^{2+}$ in an aqueous solution containing 0.10 M sodium perchlorate.

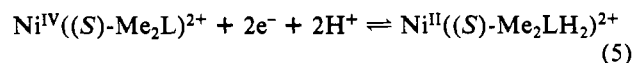
zation can occur. A different approach, involving stereospecific synthesis, was adopted.

(b) Synthesis of $\text{Ni}^{\text{II}}((S)\text{-Me}_2\text{LH}_2)^{2+}$ and $\text{Ni}^{\text{IV}}((S)\text{-Me}_2\text{L})^{2+}$. Stereospecific addition of two methyl residues to the amine backbone of the ligand LH_2 results in a sufficiently large steric interaction to form the complexes with nickel(II) and nickel(IV) stereospecifically. Chromatographic investigation of $\text{Ni}^{\text{IV}}((S)\text{-Me}_2\text{L})^{2+}$ and $\text{Ni}^{\text{II}}((S)\text{-Me}_2\text{LH}_2)^{2+}$ reveal that in both cases only one optical isomer is formed.

Spectroscopic properties of the nickel(IV) complex are similar to those of the unmethylated derivative, $\text{Ni}^{\text{IV}}\text{L}^{2+}$, although the methyl interaction causes a substantial increase in the extinction coefficient ($7500 \text{ M}^{-1} \text{ cm}^{-1}$) of the 493-nm band. Presumably this is due to a stronger overlap between metal and ligand orbitals.

The CD spectrum of $\text{Ni}^{\text{IV}}((S)\text{-Me}_2\text{L})^{2+}$, Figure 2, is similar to that of the first eluted isomer of $\text{Ni}^{\text{IV}}\text{L}^{2+}$, and the complex is likely to have the same configuration. Space-filling models support the absolute assignment proposed, and an X-ray structure determination of the corresponding nickel(II) complex is in progress.²⁰ Rotatory strengths of $\text{Ni}^{\text{IV}}\text{L}^{2+}$ and $\text{Ni}^{\text{IV}}((S)\text{-Me}_2\text{L})^{2+}$ are comparable, which suggests that, although no complete separation of $\text{Ni}^{\text{IV}}\text{L}^{2+}$ isomers proved possible with column chromatography, the first eluted isomer is close to optical purity.

(c) Redox Behavior of $\text{Ni}^{\text{IV}}((S)\text{-Me}_2\text{L})^{2+}$. The redox behavior of $\text{Ni}^{\text{IV}}((S)\text{-Me}_2\text{L})^{2+}$ was investigated with use of cyclic voltammetry at 0.10 M ionic strength (NaClO_4) and 25.0 °C in the presence of a variety of buffers ($2.0 \times 10^{-2} \text{ M}$) (Table I). At pH less than 4, a single reversible voltammetric response was noted for the reduction of $\text{Ni}^{\text{IV}}((S)\text{-Me}_2\text{L})^{2+}$. The peak-to-peak separation was approximately 30 mV at scan rates less than 20 mV s^{-1} and increased with increasing scan rate. The midpoint potential (average of the anodic and cathodic peak potentials) decreased 60 mV with each unit pH increase, indicating gain of one proton per electron in the redox process. This is consistent with eq 5 with a potential of 0.95 V (vs. NHE).



Above pH 4, the peak-to-peak separation was greater than 30 mV even at low scan rates until, around pH 5, two separate

(17) McCaffery, A. J.; Mason, S. F.; Norman, B. J.; Sargeson, A. M. *J. Chem. Soc. A* **1968**, 1304.

(18) Baucom, E. I.; Drago, R. S. *J. Am. Chem. Soc.* **1971**, *93*, 6469.

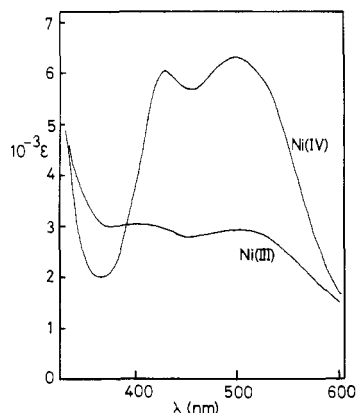
(19) Mason, S. F. *Inorg. Chim. Acta, Rev.* **1968**, *2*, 89.

(20) Lappin, A. G.; Muir, K. W.; Peacock, R. D., work in progress.

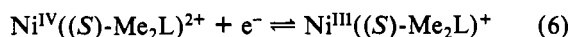
Table I. Cyclic Voltammetric Data for the $\text{Ni}^{\text{IV}}/\text{III}/\text{II}((S)\text{-Me}_2\text{L})^{2+}$ System at 25.0 °C and 0.10 M Ionic Strength (NaClO_4)

pH	$\bar{E}(\text{NHE}),^a$ V	$E_{\text{p-p}},^b$ V	$E^\circ,^c$ V	couple
1.13	0.875	0.040	0.942	(5)
1.18	0.870	0.035	0.940	(5)
1.34	0.865	0.030	0.944	(5)
1.46 ^c	0.855	0.030	0.941	(5)
2.26 ^c	0.820	0.030	0.954	(5)
2.82 ^c	0.780	0.030	0.948	(5)
3.18 ^c	0.770	0.030	0.960	(5)
3.24 ^d	0.750	0.040	0.943	(5)
3.31 ^d	0.740	0.040	0.937	(5)
4.31 ^d	0.695	0.050	0.952	(5)
4.60 ^d	0.675	0.060	0.950	(5)
4.87 ^d	0.670	0.070	0.670	(6)
5.70 ^d	0.660	e	0.660	(6)
5.97 ^d	0.660	e	0.660	(6)
	0.555	e		
6.50 ^f	0.645	0.080	0.645	(6)
	0.465	0.070		
6.79 ^f	0.655	0.075	0.655	(6)
	0.435	0.060		
7.03 ^f	0.660	0.090	0.660	(6)
	0.420	0.060	0.420	(7)
7.76 ^f	0.660	0.070	0.660	(6)
	0.425	0.080	0.425	(7)
7.80 ^f	0.660	0.070	0.660	(6)
	0.420	0.075	0.420	(7)
8.10 ^g	0.660	0.065	0.660	(6)
	0.415	0.080	0.415	(7)
8.77 ^g	0.660	0.085	0.660	(6)
	0.420	0.100	0.420	(7)
9.04 ^g	0.660	0.070	0.660	(6)
	0.425	0.105	0.425	(7)

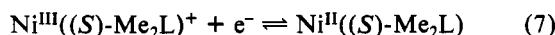
^a Average of anodic and cathodic peaks. ^b Peak-peak separation. ^c Chloroacetate buffer, 2.0×10^{-2} M. ^d Acetate buffer, 2.0×10^{-2} M. ^e Peaks overlap. ^f Phosphate buffer, 2.0×10^{-2} M. ^g Borate buffer, 2.0×10^{-2} M.

**Figure 3.** Visible absorption change induced by the reduction of $\text{Ni}^{\text{IV}}\text{L}^{2+}$ by $\text{Co}(\text{edta})^{2-}$ (1:1 ratio) at pH 8.0 to give $\text{Ni}^{\text{III}}\text{L}^+$.

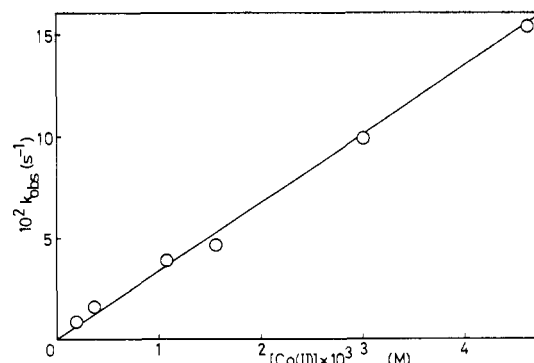
voltammetric responses could be discerned. Both responses show a peak-to-peak separation of 60 mV. The higher potential response is independent of pH with a value of 0.66 V for the reduction of nickel(IV) to nickel(III) (eq 6). The lower



potential response shows a strong (greater than 60 mV/decade) dependence between pH 5 and 6, a 60 mV/pH unit dependence between pH 6 and 7, and pH independence above pH 7. Thus, at higher pH a value of 0.42 V for eq 7 is determined.



This redox behavior of the optically active $\text{Ni}^{\text{IV}}((S)\text{-Me}_2\text{L})^{2+}$ complex is very similar to that of the unmethylated complex.^{4,5}

**Figure 4.** Plot of $k_{\text{obsd}}(1)$ against $[\text{Co}(\text{edta})^{2-}]$ for the reduction of $\text{Ni}^{\text{IV}}\text{L}^{2+}$ at 25.0 °C, 0.10 M (NaNO_3) ionic strength, and pH 6.95.**Table II.** Pseudo-First-Order Rate Constants for the Reduction of $\text{Ni}^{\text{IV}}\text{L}^{2+}$ by $\text{Co}(\text{edta})^{2-}$ at 25.0 °C and 0.10 M Ionic Strength^a

pH	$10^4 [\text{Co}(\text{edta})^{2-}],$ M	$10^2 k_{\text{obsd}}(1),$ s^{-1}
8.58 ^b	19.7	6.6 ± 0.5
6.95 ^c	1.8	0.92 ± 0.15
6.95 ^c	3.6	1.7 ± 0.1
6.95 ^c	10.8	3.9 ± 0.5
6.95 ^c	15.6	4.6 ± 0.7
6.95 ^c	30.0	9.9 ± 0.4
6.95 ^c	46.2	15.4 ± 0.4
6.58 ^d	30.8	9.9 ± 0.1
6.10 ^d	30.8	9.1 ± 1.7
5.46 ^e	19.7	6.3 ± 0.3
4.88 ^e	30.8	5.4 ± 0.8
4.06 ^e	50.0	13.5 ± 1.0

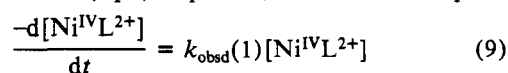
^a $[\text{Ni}^{\text{IV}}\text{L}^{2+}] = (5\text{--}7) \times 10^{-6}$ M. ^b Borate buffer, 1.5×10^{-2} M. ^c Hepes buffer, 1.5×10^{-2} M. ^d Phosphate buffer, 1.5×10^{-2} M. ^e Acetate buffer, 1.5×10^{-2} M.

(d) **Reduction of $\text{Ni}^{\text{IV}}\text{L}^{2+}$ by $\text{Co}(\text{edta})^{2-}$.** The reduction of $\text{Ni}^{\text{IV}}\text{L}^{2+}$ by $\text{Co}(\text{edta})^{2-}$ has a 1:(1.97 ± 0.07) stoichiometry at pH 4.02 consistent with eq 8. The products $\text{Co}(\text{edta})^-$ and 2H^+ + $\text{Ni}^{\text{IV}}\text{L}^{2+}$ + $2\text{Co}(\text{edta})^{2-} \rightarrow \text{Ni}^{\text{III}}\text{LH}_2^{2+} + 2\text{Co}(\text{edta})^-$ (8)

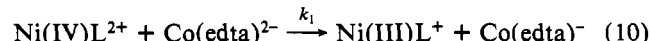
$\text{Ni}^{\text{III}}\text{LH}_2^{2+}$ were identified spectrophotometrically after separation using a cation-exchange resin. Addition of 1 equiv of $\text{Co}(\text{edta})^-$ to $\text{Ni}^{\text{IV}}\text{L}^{2+}$ at pH 8.0 results in formation of a nickel complex with the spectrum shown in Figure 3, which is approximately half the intensity of that of the nickel(IV) complex. This has been shown⁵ to be the complex $\text{Ni}^{\text{III}}\text{L}^+$ with absorption maxima at 505 nm ($2890 \text{ M}^{-1} \text{ cm}^{-1}$) and 398 nm ($3000 \text{ M}^{-1} \text{ cm}^{-1}$). There is an isobestic point for the nickel(IV)/nickel(III) interconversion at 391 nm above pH 5.

Reduction of $\text{Ni}^{\text{IV}}\text{L}^{2+}$ by $\text{Co}(\text{edta})^{2-}$ thus proceeds in two consecutive one-electron steps with formation of a nickel(III) intermediate. In conditions of excess $\text{Co}(\text{edta})^{2-}$, biphasic kinetics are observed and mechanistic details for the faster reaction, nickel(IV) reduction, and the slower reaction, nickel(III) reduction, can be evaluated independently.

(e) **Nickel(IV) Reduction Kinetics and Mechanism.** The faster reaction, corresponding to $\text{Ni}^{\text{IV}}\text{L}^{2+}$ reduction, shows good first-order behavior (eq 9) at pH > 5, where the subsequent



reaction is sufficiently slow not to interfere. A plot of $k_{\text{obsd}}(1)$ against $[\text{Co}(\text{edta})^{2-}]$ is linear (Figure 4), consistent with eq 10. At low pH, rate constants were obtained by using a



first-order consecutive reaction treatment and values of $k_{\text{obsd}}(1)$ obtained under a variety of conditions are presented in Table

Table III. Pseudo-First-Order Rate Constants for the Reduction of Ni^{III}LH²⁺ by Co(edta)²⁻ at 25.0 °C and 0.1 M Ionic Strength^a

pH	10 ³ [Co(edta) ²⁻], M	10 ³ k _{obsd}
3.56 ^b	0.51	4.9 ± 0.2
	2.40	19.6 ± 0.7
	4.00	27.2 ± 0.9
	5.00	28.3 ± 1.7
3.63 ^{c,d}	2.79	20.8 ± 0.6
	4.06 ^c	0.98
4.12 ^{c,d}	1.97	11.5 ± 0.5
	2.50	13.0 ± 0.9
	4.00	18.3 ± 0.7
	5.00	21.5 ± 0.6
	8.80	27.3 ± 0.8
	4.39	23.6 ± 0.6
	3.19	19.1 ± 0.5
4.50 ^c	0.98	6.1 ± 0.6
	4.92	15.4 ± 0.1
	9.85	19.9 ± 2.4
	5.00 ^c	0.51
6.00 ^e	2.85	6.5 ± 0.8
	3.95	9.0 ± 0.5
	5.34	9.4 ± 0.2
	7.04	8.9 ± 0.5
	7.91	13.6 ± 0.7
6.00 ^f	13.74	3.0 ± 0.1
	24.50	3.4 ± 0.1

^a [Ni^{III}L⁺]_T = (0.5–1.2) × 10⁻⁵ M. ^b Chloroacetate buffer, 3.0 × 10⁻² M. ^c Acetate buffer, 3.0 × 10⁻² M. ^d Electro-generated nickel(III). ^e Phosphate buffer, 3.0 × 10⁻² M. ^f Hepes buffer, 1.5 × 10⁻² M.

II. The second-order rate is virtually independent of pH with a second-order rate constant, $k_1 = 33 \pm 2 \text{ M}^{-1} \text{ s}^{-1}$, over the range studied although there is a slight (15%) decrease at lower pH. This may be due to inaccuracies introduced by the consecutive reaction treatment or due to protonation of Co(edta)²⁻ to yield a species that is reported²¹ as having a pK_a of 3.0.

(f) Nickel(III) Reduction Kinetics and Mechanism. At pH < 5, the slower second phase of the reaction follows first-order kinetics for greater than three half-lives, consistent with eq 11 for the decomposition of nickel(III). A plot of $k_{\text{obsd}}(2)$

$$\frac{-d[\text{Ni(III)}]}{dt} = k_{\text{obsd}}(2)[\text{Ni(III)}] \quad (11)$$

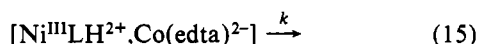
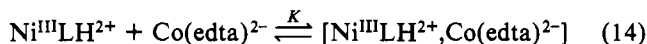
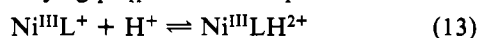
against [Co(edta)²⁻] shows limiting rate behavior, and there is also a complex pH dependence. Results obtained with electrogenerated nickel(III) were similar to those obtained by analysis of the second phase of the nickel(IV) reduction (Table III), indicating that the reactant is the same in both cases.

A good fit to all the experimental data is given by expression 12, and Figure 5 shows a plot of $k_{\text{obsd}}(2)$ against [Co-

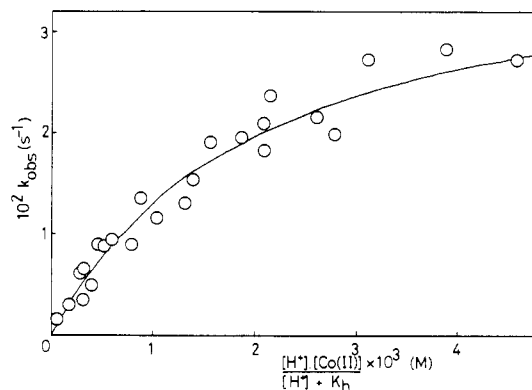
$$k_{\text{obsd}}(2) = \frac{Kk[\text{Co(edta)}^{2-}][\text{H}^+]}{K_H + [\text{H}^+](1 + K[\text{Co(edta)}^{2-}])} \quad (12)$$

(edta)²⁻][H⁺]/(K_H + [H⁺]). The solid curve is generated by the best fit parameters $k = (4.0 \pm 0.5) \times 10^{-2} \text{ s}^{-1}$, $K = 480 \pm 80 \text{ M}^{-1}$, and $K_H = (8.51 \pm 2.1) \times 10^{-5} \text{ M}$, all at 25.0 °C and 0.10 M ionic strength.

A mechanism consistent with this rate law is given in eq 13–15, thus identifying $pK_H = 4.07$ with protonation of the



nickel(III) complex. This value is in excellent agreement with

**Figure 5.** Plot of $k_{\text{obsd}}(2)$ against $[\text{H}^+][\text{Co(edta)}^{2-}]/([\text{H}^+] + K_H)$ for the reduction of Ni^{III}LH²⁺ at 25.0 °C, 0.10 M (NaNO₃) ionic strength, and pH 3.5–6.**Table IV.** Second-Order Rate Constants for the Disproportionation of Ni^{III}L⁺ at pH > 6, 25.0 °C, and 0.10 M Ionic Strength

pH	10 ³ [Co(edta) ²⁻], M	10 ⁵ [Ni ^{III} L ⁺], M	k, M ⁻¹ s ⁻¹
7.0 ^a	7.55	1.5	37 ± 3
7.0 ^a	9.81	1.5	37 ± 2
6.0 ^b	1.98	1.5	40 ± 4
			av 38 ± 3

^a Hepes buffer, 1.5 × 10⁻² M. ^b Phosphate buffer, 3.0 × 10⁻² M.

the pK_H determined in previous studies.^{5,8}

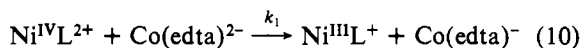
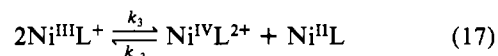
A mechanistic alternative involving rate-limiting “activation” of Ni^{III}LH²⁺ can be dismissed since such a pathway is not detected with other Ni^{III}LH²⁺ reactions⁵ although the more complex possibility that [Ni^{III}LH²⁺, Co(edta)²⁻] is a “dead-end” complex and that electron transfer takes place by eq 16 with a second-order rate constant, k_2 , of $19.2 \pm 0.8 \text{ M}^{-1} \text{ s}^{-1}$ cannot be dismissed.



Both possible mechanisms are consistent with strong complexation between Ni^{III}LH²⁺ and Co(edta)²⁻. No such interaction was detected in the reaction of Co(edta)²⁻ with the similarly charged Ni^{IV}L²⁺, and since there is little structural reorganization expected on the reduction from nickel(IV) to nickel(III), this added interaction must derive from the presence of the proton in Ni^{III}LH²⁺. Hydrogen bonding between the oxime proton and a bound carboxylate on Co(edta)²⁻ is proposed.

Oxidation of Co(edta)²⁻ by Ni^{III}L⁺ directly is apparently very slow, and an upper limit for the second-order rate constant of $5 \times 10^{-1} \text{ M}^{-1} \text{ s}^{-1}$ is consistent with the reactivity pattern of these nickel(III) species established in other studies.⁵ Attempts to measure this reaction rate at high pH are prevented by the presence of a pathway second-order in [Ni^{III}L⁺] and independent of [Co(edta)²⁻] and pH (Table IV), although at high [Co(edta)²⁻] reasonably good first-order behavior persists to pH 6.0.

The second-order pathway was not studied in great detail and is ascribed to disproportionation of Ni^{III}L⁺ that is driven by the comparatively rapid reduction of the product Ni^{IV}L²⁺ by Co(edta)²⁻ (eq 17 and 10). The derived rate expression



$$\frac{-d[\text{Ni}^{\text{III}}\text{L}^+]}{dt} = \frac{k_1 k_3 [\text{Ni}^{\text{III}}\text{L}^+]^2 [\text{Co(edta)}^{2-}]}{k_{-3} [\text{Ni}^{\text{II}}\text{L}] + k_1 [\text{Co(edta)}^{2-}]} \quad (18)$$

(21) Martell, A. E.; Smith, R. M. “Critical Stability Constants”; Plenum Press: New York, 1974; Vol. 1.

(18) reduces to the observed rate behavior if $k_{-3}[\text{Ni}^{\text{III}}\text{L}]$ is less than $k_1[\text{Co}(\text{edta})^{2-}]$, which is true provided studies are carried out in the pH range where the nickel(II) complex is protonated. The range of conditions is limited due to deviations from second-order behavior at higher $[\text{Co}(\text{edta})^{2-}]$ introduced by the first-order acid-catalyzed pathway. Values for $k_3 = 38 \pm 3 \text{ M}^{-1} \text{ s}^{-1}$, $k_{-3} = (3 \pm 2) \times 10^5 \text{ M}^{-1} \text{ s}^{-1}$, and $k_1 = 33 \pm 2 \text{ M}^{-1} \text{ s}^{-1}$ are calculated from the available kinetic and thermodynamic data.

(g) **Marcus Considerations.** The nickel(IV) complex $\text{Ni}^{\text{IV}}\text{L}^{2+}$ is substitution inert and is likely to undergo electron-transfer reactions by outer-sphere mechanisms. A nickel(IV)/nickel(III) self-exchange rate constant of $3 \times 10^5 \text{ M}^{-1} \text{ s}^{-1}$ is evaluated from the present work with use of eq 19 and 20, where Z is the collision number for neutral molecules

$$k_{12} = (k_{11}k_{22}K_{12}f)^{1/2} \quad (19)$$

$$\log f = (\log K_{12})^2 / 4 \log (k_{11}k_{22}Z^{-2}) \quad (20)$$

in solution, $10^{11} \text{ M}^{-1} \text{ s}^{-1}$. This is in good agreement with a value of $\sim 1 \times 10^5 \text{ M}^{-1} \text{ s}^{-1}$ determined previously⁵ in the reduction by $\text{Co}(\text{phen})_3^{2+}$. The reactants $\text{Co}(\text{phen})_3^{2+}$ and $\text{Co}(\text{edta})^{2-}$ are oppositely charged, and at the ionic strength employed in these studies, electrostatic effects can be important. Electrostatics-corrected self-exchange rate constants²² are in poorer agreement with a value of $9 \times 10^4 \text{ M}^{-1} \text{ s}^{-1}$ derived from the $\text{Co}(\text{phen})_3^{2+}$ data and $2 \times 10^4 \text{ M}^{-1} \text{ s}^{-1}$ derived from the $\text{Co}(\text{edta})^{2-}$ data. Nevertheless, they remain within experimental error.

Nickel(III) complexes may exhibit considerable substitution lability, and so outer-sphere mechanisms in their reactions with $\text{Co}(\text{edta})^{2-}$ cannot be assumed but are considered probable.⁵ Marcus calculations based on the second-order rate constant Kk of $19.2 \text{ M}^{-1} \text{ s}^{-1}$ give a value of $1 \times 10^5 \text{ M}^{-1} \text{ s}^{-1}$ for the $\text{Ni}^{\text{III}}\text{LH}^{2+}/\text{Ni}^{\text{III}}\text{LH}^+$ self-exchange, considerably in excess of the value of $1 \times 10^3 \text{ M}^{-1} \text{ s}^{-1}$ suggested previously.⁵ This may be a consequence of the strong precursor complex formation, which is specific to the cross reaction.²³

With use of a value of $2 \times 10^3 \text{ M}^{-1} \text{ s}^{-1}$ for the $\text{Ni}^{\text{III}}\text{L}^+/\text{Ni}^{\text{III}}\text{L}^0$ self-exchange,⁵ an estimate for the unmeasured rate of reduction of $\text{Ni}^{\text{III}}\text{L}^+$ by $\text{Co}(\text{edta})^{2-}$ of $2 \times 10^{-3} \text{ M}^{-1} \text{ s}^{-1}$ can be obtained and this is within the experimental error of the data. The second-order pathway, which is dominant at high pH, yields a value of $4.5 \times 10^3 \text{ M}^{-1} \text{ s}^{-1}$ for the $\text{Ni}^{\text{III}}\text{L}^+/\text{Ni}^{\text{III}}\text{L}^0$ self-exchange, which is reasonably consistent with other estimates of this parameter.⁵

(h) **Stereoselectivity.** The presence of additional methyl groups in $\text{Ni}^{\text{II}}((S)\text{-Me}_2\text{L})^{2+}$ is unlikely to affect markedly the reactivity pattern of nickel(IV) reduction by $\text{Co}(\text{edta})^{2-}$ as outlined for $\text{Ni}^{\text{IV}}\text{L}^{2+}$. Indeed, reduction potentials for the two complexes are similar. However, in the determination of reaction stereoselectivity, the complex $\text{Ni}^{\text{IV}}((S)\text{-Me}_2\text{L})^{2+}$ has distinct advantages over $\text{Ni}^{\text{IV}}\text{L}^{2+}$, particularly the retention of the configuration in the reduced nickel complexes. Experiments performed under a variety of conditions allow a strong indication of the stereospecificity of the reaction pathways outlined above (Table V).

(1) At pH 6.13 and ionic strength 0.10 M, with $[\text{Ni}^{\text{IV}}((S)\text{-Me}_2\text{L})^{2+}]:[\text{Co}(\text{edta})^{2-}] = 1:1$, the specificity of the nickel(IV) reduction step (10) is determined as $11 \pm 0.5\%$.

(2) At pH 6.13 and ionic strength 0.10 M, with $[\text{Ni}^{\text{IV}}((S)\text{-Me}_2\text{L})^{2+}]:[\text{Co}(\text{edta})^{2-}] = 1:2$, the combined specificity

Table V. Results of Stereoselectivity Experiments at 25.0 °C in Acetate Media

$[\text{Ni}^{\text{IV}}((S)\text{-Me}_2\text{L})^{2+}]$, M	$[\text{Co}(\text{edta})^{2-}]$, M	pH	μ , M	% [(+)- Co(edta) ²⁻] excess
6.8×10^{-4}	6.8×10^{-4}	6.13	0.10	11.0 ± 0.5
6.8×10^{-4}	1.36×10^{-4}	6.13	0.10	11.1 ± 0.5
6.8×10^{-4}	1.36×10^{-4}	4.02	0.10	10.6 ± 0.5
6.8×10^{-5}	1.36×10^{-5}	4.02	0.01	10.0 ± 0.5

of step 10 and the pathway (17) and (10) was found to be $11.1 \pm 0.5\%$. Since the oxidation of $\text{Co}(\text{edta})^{2-}$ occurs only by step 10, the similarity of the results in (1) and (2) is encouraging.

(3) At pH 4.02 and ionic strength 0.10 M, with $[\text{Ni}^{\text{IV}}((S)\text{-Me}_2\text{L})^{2+}]:[\text{Co}(\text{edta})^{2-}] = 1:2$, the combined specificity of step 10 and the pathway (13) and (14) is $10.6 \pm 0.5\%$, which implies that stereoselectivity of the nickel(III) reduction is around 10%, close to the value for nickel(IV) reduction. The overall stereoselectivity under these conditions is little changed ($10.0 \pm 0.5\%$) by reducing the ionic strength by a factor of 10.

Stereoselectivity in outer-sphere electron-transfer reactions can originate from two sources: induced stereochemical preference in the precursor complex (Pfeiffer effect), which is unlikely in these reactions of oligodentate chelates where partial unwrapping of the ligand is required to change from one configuration to another, and alternatively, and in this case more likely, preferential precursor complex formation with one optical isomer or preferential orbital overlap leading to more rapid electron transfer with one optical isomer than with the other.

The similarity in stereoselectivity of the nickel(IV) and nickel(III) reactions in spite of the differences in precursor complex formation is of interest. Both nickel complexes have similar structure and chirality, and though the detailed interactions with $\text{Co}(\text{edta})^{2-}$ are clearly quite different in the two cases, stereoselectivity, which is determined by the chiral nature of the oxidant, is similar. Thus, no matter the absolute magnitude of the precursor association constant, the preference for one isomer over the other remains approximately constant. This is reinforced by the experiment at lower ionic strength, where stereoselectivity is unaltered but complex formation might be expected to be enhanced.

Conclusions

Reduction of the nickel(IV) oxime–imine complex $\text{Ni}^{\text{IV}}\text{L}^{2+}$ by $\text{Co}(\text{edta})^{2-}$ proceeds by an initial pH-independent, outer-sphere one-electron transfer to form $\text{Ni}^{\text{III}}\text{L}^+$. Protonation of the nickel(III) complex to form $\text{Ni}^{\text{III}}\text{LH}^{2+}$ results in further reduction with formation of the hydrogen-bonded intermediate complex $[\text{Ni}^{\text{III}}\text{LH}^{2+}, \text{Co}(\text{edta})^{2-}]$. The complex $\text{Ni}^{\text{III}}\text{L}^+$ does not react directly with $\text{Co}(\text{edta})^{2-}$ but undergoes disproportionation. Stereoselectivity in this reaction was investigated with use of a stereospecifically produced dimethyl derivative of the nickel(IV) reagent and is around 10% in each step. It is concluded that the stereoselectivity is determined mainly by the chirality of the participating reagents and not by the strength of precursor complex formation.

Acknowledgment. We thank the SERC for a grant to purchase a stopped-flow spectrophotometer and to construct a CD apparatus, CAPES, Brazil, for a maintenance grant (M.C.M.L.), and Mr. Barry Thomson and Mr. Paul J. Heaney for some technical assistance.

Registry No. $\text{Ni}^{\text{II}}\text{LH}_2(\text{ClO}_4)_2$, 55188-32-4; $\text{Ni}^{\text{III}}\text{L}(\text{ClO}_4)$, 84370-58-1; $\text{Ni}^{\text{IV}}\text{L}(\text{ClO}_4)_2$, 55188-34-6; (S)- Me_2LH_2 , 84370-59-2; $\text{Ni}^{\text{II}}((S)\text{-Me}_2\text{LH}_2)(\text{NO}_3)_2$, 84370-61-6; $\text{Ni}^{\text{IV}}((S)\text{-Me}_2\text{L})^{2+}$, 84370-62-7; $\text{Co}(\text{edta})^{2-}$, 14931-83-0; $\text{Ni}^{\text{III}}((S)\text{-Me}_2\text{L})^+$, 84370-63-8; $\text{Ni}^{\text{III}}\text{LH}^{2+}$, 83875-36-9; (-)- $\text{Co}(\text{edta})^-$, 27829-16-9; (+)- $\text{Co}(\text{edta})^-$, 18661-70-6.

(22) Calculations followed: Brown, G. M.; Sutin, N. *J. Am. Chem. Soc.* **1979**, *101*, 883. Ionic radii were estimated from available structural data to be as follows: $\text{Co}(\text{edta})^{-/2-}$, 5 Å; $\text{Co}(\text{phen})_3^{3+/2+}$, 7 Å; $\text{NiL}^{2+/+}$, 6 Å.

(23) Marcus, R. A.; Sutin, N. *Inorg. Chem.* **1975**, *14*, 213.